Pythagorean Hodograph Curves: A Survey of Recent Advances

Jiří Kosinka
Computer Laboratory
University of Cambridge
Jiri.Kosinka@cl.cam.ac.uk

Miroslav Lávička
NTIS
University of West Bohemia
Lavicka@kma.zcu.cz

Abstract: Pythagorean hodograph (PH) curves, defined by Farouki and Sakkalis in 1990, and their applications in offsetting, CNC machining, motion planning etc., have become an active research area in recent years. These curves (and other objects with a Pythagorean property) have fascinated many researchers and one can find hundreds of papers devoted to this beautiful topic. An early survey on PH curves was done by Farouki in Section 17 of the Handbook of Computer Aided Geometric Design (2002). In 2008, a special issue of the journal CAGD was devoted to "Pythagorean-hodograph curves and related topics". A unified introduction to existing material on shapes with the Pythagorean property and also new research starting points were described in the book by Farouki in the same year. This book can also serve as a detailed survey of the literature concerning PH curves and related topics. However, development never stops and recent years have seen further intensive investigation in the field of PH curves. This paper tries to summarise research on PH curves over the last years in three major strands: polynomial PH curves, rational PH curves, and Hermite interpolation by PH curves in Euclidean and Minkowski plane and space.

Keywords: Pythagorean hodograph curves, rational offsets, interpolation.

1 Introduction

Shapes in Computer Aided Design (CAD), and in a vast variety of geometrical applications, are often described by piecewise rational representations (for more details see [23] and references therein). However, not every shape (curve, surface, volume) can be described using rational parametrisations, see [95] for more details. Another major problem of CAD is that many natural geometrical operations, such as convolution [98], construction of Minkowski sums, and especially offsetting, do not preserve rationality of derived objects. This is the main reason why approximate techniques, which generate a rational parametrisation within a certain region of interest, and related algorithms have been studied extensively.

On the other hand, offsets to certain special classes of curves admit exact rational representations. In the case of planar curves, the class of Pythagorean hodograph (PH) curves as polynomial curves possessing rational offset curves and polynomial arc-length functions was introduced in [31]. A thorough analysis of PH curves followed; see e.g. [29, 58, 84]. Later, the concept of polynomial planar PH curves was generalised to polynomial spatial PH curves [32, 33], to rational planar PH curves [90, 91, 88], and recently also to rational spatial PH curves [47]. The case of PH curves in $\mathbb{R}^n$ for $n > 3$ is still not solved satisfactorily. Nevertheless, exploiting recent results from number theory, the structure of PH curves in dimensions $n = 5$ and $n = 9$ was characterized in [93, 92].

Even though PH curves possess rational offsets, the usually most costly ingredient, the trimming, still needs to be performed as in the case of approximating techniques. An alternative approach to this problem based on the medial axis transform (MAT) of a planar domain, introduced in [10], was formulated in [82] and [19]. There exists a one-to-one correspondence between the MAT in three-dimensional Minkowski space $\mathbb{R}^{2,1}$ and the object boundary. The main advantages of this description follow from the dimensional reduction while topological properties are maintained. As observed in [82, 19], if a segment of the medial axis transform is an MPH (Minkowski Pythagorean hodograph) curve, then the associated branches of the domain boundaries are segments of rational curves. In addition, all offsets of the domain boundary possess this property as well. A thorough analysis of MPH curves followed; see e.g. [14, 15, 16, 60]. Recently, polynomial MPH curves were generalised to rational MPH curves in [67, 68].

However, focusing only on the fact that PH curves possess rational offsets does not give a full overview of their useful properties. Another very important practical application is based on the fact that the parametric speed of polynomial PH curves is polynomial. This is important for formulating efficient real time interpolator algorithms for CNC machines. Let us recall that the interpolators for general NURBS curves are typically computed using Taylor series expansions. Of course, this approach brings truncation errors caused by omitting higher-order terms.

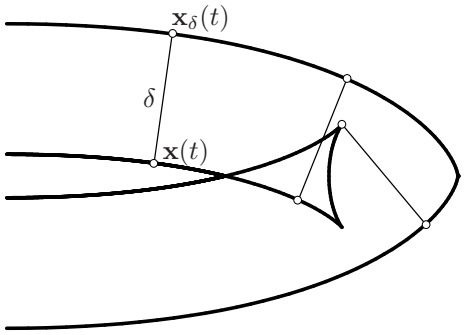

Figure 1: The offset $\mathbf{x}_\delta(t)$ of $\mathbf{x}(t)$ at distance δ.

When the Pythagorean hodograph curves are applied for describing the tool path, this problem is overcome, see e.g. [46, 96, 80].

This survey summarises recent work on PH curves in three major strands:

- polynomial PH curves (Sections 2 and 3),
- rational PH curves (Sections 2 and 4),
- Hermite interpolation by PH curves (Section 5).

Within this scope, re-emerging topics include rational rotation minimising frames (Section 3.2) and double PH curves (Section 3.3). Further recent research on PH curves and their applications includes [3, 61, 105, 81].

Results on surfaces with certain Pythagorean properties fall beyond the scope of the present survey. We refer the reader interested in Pythagorean normal vector surfaces (shortly PN surfaces) and their generalisation to MOS surfaces (i.e., Medial surfaces Obeying the Sum of squares condition) to [90] (see also [72, 75, 76] for more details) and [65] (see also [87, 86, 85] for further information and [7, 6] for applications), respectively.

2 Planar PH curves

In this section we briefly review the fundamentals of offsets (see Fig. 1) and polynomial and rational curves with Pythagorean hodographs in the Euclidean plane.

Given a regular C^1 parametric curve $\mathbf{x}(t) = (x_1(t), x_2(t))^\top$, the *offset* of $\mathbf{x}(t)$ is the set of all points in $\mathbb{R}^2$ that lie at a distance δ from $\mathbf{x}(t)$. The two branches of the offset are given by

$$\mathbf{x}_\delta(t) = \mathbf{x}(t) \pm \delta\,\mathbf{n}(t), \qquad \mathbf{n}(t) = \frac{\mathbf{x}'(t)^\perp}{\|\mathbf{x}'(t)\|}, \tag{1}$$

where $\|\mathbf{x}'(t)\| = \sqrt{x_1'(t)^2 + x_2'(t)^2}$ and $\mathbf{x}'(t)^\perp = (-x_2'(t), x_1'(t))^\top$, i.e., $\mathbf{v}^\perp$ denotes the rotation of $\mathbf{v} \in \mathbb{R}^2$ about the origin by the angle $+\frac{\pi}{2}$.

Offset curves are used mainly in numerically controlled machining. They describe a round cutting tool path, which is parallel to the cut at a constant distance in direction normal to the cut at every point. However, even for rational $\mathbf{x}(t)$ the rationality of its offsets is generally not guaranteed. A study of offset rationality led to the class of planar *Pythagorean hodograph* (PH) curves. These curves are defined as rational curves $\mathbf{x}(t) = (x_1(t), x_2(t))^\top$ satisfying the PH condition

$$\mathbf{x}'(t) \cdot \mathbf{x}'(t) = x_1'(t)^2 + x_2'(t)^2 = \sigma(t)^2, \tag{2}$$

where $\sigma(t)$ is a rational function, i.e., an element of $\mathbb{R}(t)$, and '$\cdot$' is the standard Euclidean inner product. Since the rationality of the δ-offset curve $\mathbf{x}_\delta(t)$ of a rational curve depends only on the rationality of the unit normal field $\mathbf{n}(t)$, cf. (1), planar PH curves possess (piece-wise) rational offsets.

Pythagorean hodograph curves were originally introduced in [31] as *planar polynomial* curves. It was proved in [31, 73] that the coordinates of hodographs of polynomial PH curves and $\sigma(t)$ form the following Pythagorean triples

$$\begin{aligned} x_1'(t) &= w(t)\big(u^2(t) - v^2(t)\big), \\ x_2'(t) &= 2w(t)u(t)v(t), \\ \sigma(t) &= w(t)(u^2(t) + v^2(t)), \end{aligned} \tag{3}$$

where $u(t)$, $v(t)$, $w(t) \in \mathbb{R}[t]$ are any non-zero polynomials and $u(t), v(t)$ are relatively prime. The parametrisation of the PH curve is then obtained by integrating the hodograph coordinates from (3).

Remark 2.1 *In order to avoid working with piece-wise representations, it is customary to consider only curves for which $\sigma(t) > 0$ in the interval of interest. Then, $\sigma(t)$ is called* speed *of $\mathbf{x}(t)$. This is merely a technical assumption not affecting generality. In cases when $\sigma(t) < 0$, one can either substitute $-w(t)$ for $w(t)$ in* (3) *or consider $|\sigma(t)|$ instead of $\sigma(t)$.*

A generalisation of planar polynomial PH curves to rational ones was introduced and studied in [90]. As the integrals of rational functions are not rational functions in general, one cannot use formulae (3) and a different approach for describing rational PH curves must be applied. This approach uses the dual representation of a planar curve considered as an envelope of its tangents

$$n_1(t)x_1 + n_2(t)x_2 = h(t), \qquad n_1(t), n_2(t), h(t) \in \mathbb{R}(t). \tag{4}$$

In order to guarantee the rationality of (1), the unit normal field $\mathbf{n}(t)$ must rationally parametrise the unit circle. Hence, there must exist relatively prime polynomials $k(t), l(t)$ such that

$$n_1(t) = \frac{2k(t)l(t)}{k^2(t) + l^2(t)}, \quad n_2(t) = \frac{k^2(t) - l^2(t)}{k^2(t) + l^2(t)}. \tag{5}$$

For the sake of brevity we omit the dependence on parameter t and write simply $\mathbf{x}$ instead of $\mathbf{x}(t)$, k instead of $k(t)$, etc., whenever no confusion is likely to arise. To simplify further computations, we set $g = h(k^2 + l^2)$, i.e., the dual representation of an arbitrary PH curve is

$$(2kl : k^2 - l^2 : -g). \tag{6}$$

Consequently, a parametric representation of all planar rational PH curves is obtained as the envelope of their tangents given by (6). We recall that the planar rational and polynomial PH curves were related in [42] where it was shown how to choose $k(t)$, $l(t)$, $g(t)$ to obtain polynomial PH curves from the envelope formula for rational PH curves.

Furthermore, the representation of offsets can be obtained easily by translating the tangents by a distance δ, i.e., it is sufficient to replace $g(t) = h(t)(k(t)^2 + l(t)^2)$ by $g(t) = (h(t) \pm \delta)(k(t)^2 + l(t)^2)$.

Remark 2.2 *Since planar Minkowski PH curves seem to have only limited applicability, we refer the reader to [63, 24] for more details.*

3 Spatial polynomial PH and MPH curves

Now we recall the basics of polynomial PH curves both in Euclidean and Minkowski space.

3.1 Polynomial PH curves in Euclidean space

The concept of planar polynomial PH curves was generalised to 3-dimensional Euclidean space in [32]. By analogy with [31], a polynomial spatial PH curve $\mathbf{x}(t) = (x_1(t), x_2(t), x_3(t))^\top$ is characterised by the condition

$$\mathbf{x}'(t) \cdot \mathbf{x}'(t) = x_1'(t)^2 + x_2'(t)^2 + x_3'(t)^2 = \sigma(t)^2, \tag{7}$$

where $\sigma(t)$ is a polynomial.

Similarly to (3), (7) invokes a characterization of the hodograph components in terms of four polynomials. In particular, a *spatial polynomial* curve is a (Euclidean) Pythagorean hodograph curve if and only if its hodograph can be expressed in the form

$$\begin{aligned} x_1' &= U^2 - V^2 - P^2 + Q^2, \\ x_2' &= 2UV + 2PQ, \\ x_3' &= 2UP - 2VQ, \\ \sigma &= \pm(U^2 + V^2 + P^2 + Q^2), \end{aligned} \tag{8}$$

where $U, V, P, Q \in \mathbb{R}[t]$, see [32]. This representation is based on the generalised stereographic projection, see [22].

Spatial Pythagorean hodograph curves have the following attractive properties:

- the arc length of any segment can be determined exactly without numerical approximation,
- they possess rational adapted frames.

For more details about practical applications of spatial PH curves see [24] and references therein.

Finally, we recall the quaternion representation (see [5] for more details about quaternions) of polynomial spatial PH curves. Given a quaternion polynomial

$$\mathcal{A}(t) = U(t) + V(t)\mathbf{i} + P(t)\mathbf{j} + Q(t)\mathbf{k} \tag{9}$$

of degree d, the hodograph

$$\mathbf{x}'(t) = \mathcal{A}(t)\mathbf{i}\mathcal{A}^*(t), \tag{10}$$

where $\mathcal{A}^*(t) = U(t) - V(t)\mathbf{i} - P(t)\mathbf{j} - Q(t)\mathbf{k}$, has the form (8), i.e., it defines a PH curve of degree $2d+1$, see [16].

3.2 PH curves and rational rotation-minimising frames

An *adapted frame* on a regular spatial curve $\mathbf{x}(t)$ is an orthonormal basis $(\mathbf{e}_1, \mathbf{e}_2, \mathbf{e}_3)$ in $\mathbb{R}^3$ such that $\mathbf{e}_1$ coincides with $\mathbf{t} = \mathbf{x}'/\|\mathbf{x}'\|$ at each point. The *Frenet frame* $(\mathbf{t}, \mathbf{n}, \mathbf{b})$, where

$$\mathbf{t} = \frac{\mathbf{x}'}{\|\mathbf{x}'\|}, \quad \mathbf{n} = \frac{\mathbf{x}' \times \mathbf{x}''}{\|\mathbf{x}' \times \mathbf{x}''\|} \times \mathbf{t}, \quad \mathbf{b} = \mathbf{t} \times \mathbf{n} \tag{11}$$

are the unit tangent, normal, and binormal vector, respectively, is one of the best known adapted frames. The variation of an adapted frame along a curve $\mathbf{x}(t)$ is given by the angular velocity $\boldsymbol{\omega}(t)$. We recall that the *angular velocity* of a frame is a vector whose magnitude describes the instantaneous angular speed and the direction gives the axis of rotation. The derivatives of the frame vectors can be expressed in terms of the frame angular velocity as

$$\mathbf{e}_1' = \boldsymbol{\omega} \times \mathbf{e}_1, \quad \mathbf{e}_2' = \boldsymbol{\omega} \times \mathbf{e}_2, \quad \mathbf{e}_3' = \boldsymbol{\omega} \times \mathbf{e}_3. \tag{12}$$

The distinguishing property of a *rotation-minimising frame* (RMF) is that there is no instantaneous rotation of $\mathbf{e}_2, \mathbf{e}_3$ along $\mathbf{t} = \mathbf{e}_1$, i.e., the angular velocity $\boldsymbol{\omega}(t)$ has no component along $\mathbf{t}$. The Frenet frame is not rotation-minimising. The RMFs have important applications in computer graphics, animation and motion control.

Choi and Han [18] introduced the *Euler-Rodriques frame* (ERF) consisting of the vectors

$$\mathbf{t}(t) = \frac{\mathcal{A}(t)\mathbf{i}\mathcal{A}(t)^*}{\mathcal{A}(t)\mathcal{A}^*(t)}, \; \mathbf{u}(t) = \frac{\mathcal{A}(t)\mathbf{j}\mathcal{A}(t)^*}{\mathcal{A}(t)\mathcal{A}^*(t)}, \; \mathbf{v}(t) = \frac{\mathcal{A}(t)\mathbf{k}\mathcal{A}(t)^*}{\mathcal{A}(t)\mathcal{A}^*(t)} \tag{13}$$

as an alternative to the Frenet frame defined on spatial PH curves determined by (9). Despite the fact that this frame depends on the coordinate system, it brings an additional important advantage: it is rational as PH curves have rational unit tangent vectors. And compared to the Frenet frame, it is non-singular at inflections.

The conditions under which ERFs are RMFs were thoroughly investigated in [18]. In particular

- for PH cubics the Frenet frame and ERF are the same,
- for PH quintics, the ERF is an RMF only for planar curves,
- spatial PH curves having ERF as RMF are of degree at least 7.

Curves with rational rotation-minimising frames (RRMFs) form a proper subset of PH curves. RRMFs on PH quintics were investigated in [38, 35, 44, 45, 25]. Cubics and general degree PH curves were treated in [53, 43]. It turns out that

- PH cubics with RRMFs are either linear or planar,
- spatial PH curves with RRMFs are of degree at least 5.

In a recent paper [71], the authors presented an interpolation of data points and rotations at the points with spatial quintic PH curves so that the Euler-Rodrigues frame of the curve coincides with the rotations at the points. Further, rigid body motions using rational rotation-minimising frames were investigated in [48]. Recently, a closely related topic to RRMFs was studied in [26]; in this paper the authors investigated rotation-minimising osculating frames (RMOFs) on double PH curves which possess not only rational tangent vectors but the whole rational Frenet frame, curvature, and torsion. Double PH curves are shortly discussed in the next section.

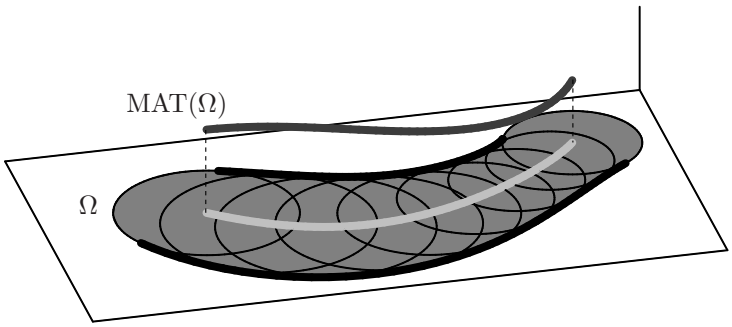

Figure 2: A domain Ω, its maximal inscribed discs, $\mathrm{MA}(\Omega)$ (light grey) and $\mathrm{MAT}(\Omega)$ (dark grey).

3.3 Double PH curves

A distinguishing property of a spatial PH curve $\mathbf{x}(t)$ is that its unit tangent vector $\mathbf{t}$ is rational in t. However, the unit normal vector $\mathbf{n}$ and binormal vector $\mathbf{b}$ are not, since they depend on $\|\mathbf{x}' \times \mathbf{x}''\|$, cf. (11). Further, while the torsion of $\mathbf{x}(t)$

$$\tau(t) = \frac{(\mathbf{x}' \times \mathbf{x}'') \cdot \mathbf{x}''}{\|\mathbf{x}' \times \mathbf{x}''\|^2} \tag{14}$$

is rational, the curvature

$$\kappa(t) = \frac{\|\mathbf{x}' \times \mathbf{x}''\|}{\|\mathbf{x}'\|^3} \tag{15}$$

is generally not. Hence, investigation of the existence of curves for which $(\mathbf{t}, \mathbf{n}, \mathbf{b})$ and κ, τ are all rational in the curve parameter led to the class of double Pythagorean hodograph (DPH) curves, for which it holds simultaneously

$$\|\mathbf{x}'\|^2 = \sigma^2, \quad \text{and} \quad \|\mathbf{x}' \times \mathbf{x}''\|^2 = (\sigma\omega)^2, \tag{16}$$

for some polynomials $\sigma(t), \omega(t) \in \mathbb{R}[t]$. This structure was first identified in [41] and its importance was emphasised by investigations in [9]. Using the quaternion representation, see (9), the DPH condition requires that the polynomials $U(t), V(t), P(t), Q(t)$ in addition fulfill

$$\begin{aligned} UP' - U'P + VQ' - V'Q &= h(a^2 - b^2), \\ UQ' - U'Q - VP' + V'P &= 2hab, \\ \omega &= 2h(a^2 + b^2), \end{aligned} \tag{17}$$

where $a(t), b(t), h(t) \in \mathbb{R}[t]$, $\gcd(a, b) = 1$.

As observed in [41], all helical polynomial curves are PH curves (helices are characterized by the property that their unit tangents maintain a constant inclination with respect to a fixed line, the axis of the helix). And as for a helical polynomial curve the quantity $\|\mathbf{x}' \times \mathbf{x}''\|$ is a polynomial in t, every helical PH curve is a DPH curve. Later, it was shown in [9] that for cubics and quintics, there is an exact coincidence of helical curves and DPH curves. Moreover, the simplest double PH curves that are non-helical are of degree 7. For further results on PH helices and DPH curves see [39, 40, 54, 55].

3.4 Medial axis transforms with rational domain boundaries

Consider a planar domain $\Omega \subset \mathbb{R}^2$ and the family of all inscribed discs in Ω partially ordered with respect to inclusion, see Fig. 2. An inscribed disc is called maximal if it is not contained in any other inscribed disc. Then the *medial axis* $\mathrm{MA}(\Omega)$ is the locus of all centres $(y_1, y_2)^\top$ of maximal inscribed discs and the *medial axis transform* $\mathrm{MAT}(\Omega)$ is obtained by appending the corresponding disc radii y_3 to the medial axis, i.e., $\mathrm{MAT}(\Omega)$ consists of points $\mathbf{y} = (y_1, y_2, y_3)^\top$. The projection

$$\mathbb{R}^{2,1} \to \mathbb{R}^2 : \quad \mathbf{y} = (y_1, y_2, y_3)^\top \mapsto \breve{\mathbf{y}} = (y_1, y_2)^\top \tag{18}$$

naturally relates $\mathrm{MAT}(\Omega)$ to $\mathrm{MA}(\Omega)$.

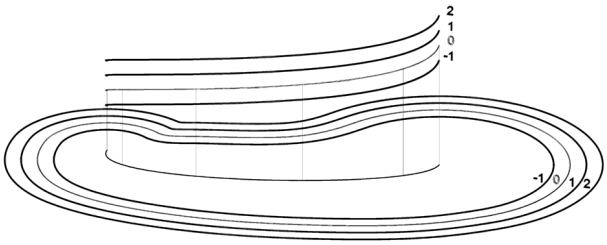

Figure 3: Offsets of a domain can be obtained by lifting its MAT.

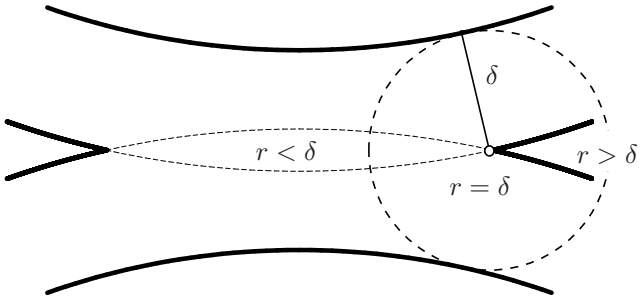

Figure 4: Trimming using the medial axis transform.

For a given geometric object there is a unique MAT. Conversely, the boundary of an object can be reconstructed from its MAT as the envelope of the one-parameter family of discs.

The notion of MAT can be generalised to non-closed shapes. For example for two curve segments (see Fig. 2), maximal discs are replaced with discs touching both segments. The notions MA and MAT are used in this broader sense.

For a C^1 segment $\mathbf{y}(t) = (y_1, y_2, y_3)^\top$ of $\mathrm{MAT}(\Omega)$ one can compute the corresponding boundary of Ω using the envelope formula [19, 82] in the form

$$\mathbf{x}_\pm = \overset{\triangledown}{\mathbf{y}} - \frac{y_3}{{y_1'}^2 + {y_2'}^2} \left(y_3' \overset{\triangledown}{\mathbf{y}}{}' \pm \sqrt{{y_1'}^2 + {y_2'}^2 - {y_3'}^2}\, \overset{\triangledown}{\mathbf{y}}{}'^{\perp} \right). \tag{19}$$

Let $\mathbf{y} \subset \mathbb{R}^{2,1}$ be a curve considered as the MAT of a planar domain and let $\mathbf{x}_\pm \subset \mathbb{R}^2$ be given by the envelope formula (19). Then $\mathbf{x}_+$ and $\mathbf{x}_-$ are called *associated* with $\mathbf{y}$.

The property of $\mathbf{x}_\pm$ being associated with $\mathbf{y}$ can be generalised to the family of translated copies of $\mathbf{y}$ in the y_3-direction and the corresponding δ-offsets of $\mathbf{x}_\pm$; see Fig. 3. We note that $\mathbf{x}_\pm$ are also known as the components of the cyclographic image of $\mathbf{y}$ in the context of Laguerre geometry; see [88, 91].

We emphasise that using the MAT representation makes the trimming procedure for the inner offsets very simple; see Fig. 4. Only those parts of the MAT where the corresponding circle/sphere radius r is less than the offset distance δ have to be trimmed [13, 12, 1].

A study of rationality of envelopes (19) led to the class of *Minkowski Pythagorean hodograph* (MPH) curves introduced as polynomial curves in [82]. Later in [67], MPH curves were generalised to *rational* curves $\mathbf{y} = (y_1, y_2, y_3)^\top$ in three-dimensional space satisfying the condition

$${y_1'}^2 + {y_2'}^2 - {y_3'}^2 = \varrho^2, \tag{20}$$

where $\varrho \in \mathbb{R}(t)$. The PH condition (7) now holds with respect to the indefinite *Minkowski inner product*

$$\langle \mathbf{u}, \mathbf{v} \rangle = u_1 v_1 + u_2 v_2 - u_3 v_3. \tag{21}$$

This fact makes the *Minkowski space* $\mathbb{R}^{2,1}$ the natural ambient space for MPH curves.

Analogously to the Euclidean case, a necessary and sufficient condition for a *spatial polynomial* curve to possess a Minkowski Pythagorean hodograph can be expressed in the form

$$\begin{array}{rcl} y_1' &=& U^2 - V^2 + P^2 - Q^2, \\ y_2' &=& 2UV - 2PQ, \\ y_3' &=& 2UP - 2VQ, \\ \varrho &=& U^2 + V^2 - P^2 - Q^2, \end{array} \tag{22}$$

where $U, V, P, Q \in \mathbb{R}[t]$, see [82]. In order to simplify computations, this formula was later modified to

$$\begin{array}{rclrcl} y_1' &=& bd - ac, & y_2' &=& bc + ad, \\ y_3' &=& bc - ad, & \varrho &=& bd + ac \end{array} \tag{23}$$

by setting

$$a = V - P, \quad b = U - Q, \quad c = V + P, \quad d = U + Q \tag{24}$$

in (22), see [67]. Again, as in the case of PH curves (cf. Remark 2.1), the restriction to $\varrho(t) > 0$ gives rise to *Minkowski speed* $\varrho(t)$.

Using (23), the envelope formula for polynomial MPH curves has the closed form

$$\begin{array}{rcl} \mathbf{x}_+ &=& \overset{\triangledown}{\mathbf{y}} + \dfrac{y_3}{a^2 + b^2} \begin{pmatrix} 2ab \\ a^2 - b^2 \end{pmatrix}, \\ \mathbf{x}_- &=& \overset{\triangledown}{\mathbf{y}} - \dfrac{y_3}{c^2 + d^2} \begin{pmatrix} 2cd \\ c^2 - d^2 \end{pmatrix}. \end{array} \tag{25}$$

We emphasise that (22) or (23) as well as its Euclidean counterpart (8) do not extend in a natural way to rational (M)PH curves. This is due to the fact that one needs to integrate the hodograph to obtain the curve itself. Indeed, integrating a general rational function does not yield a rational result.

4 Rational Euclidean and Minkowski spatial PH curves

In this section we summarise main known results on rational PH curves in Euclidean and Minkowski space and propose a unifying framework.

4.1 Rational Euclidean spatial PH curves

A method for constructing rational spatial PH curves has been recently proposed in [47]. It is known that at each point of a spatial curve $\mathbf{x}(t)$ one can construct the normal, rectifying, and osculating planes, whose points $\mathbf{p} = (x, y, z)^\top$ satisfy

$$\begin{array}{rcl} \mathbf{t}(t) \cdot \big(\mathbf{p} - \mathbf{x}(t)\big) &=& 0, \\ \mathbf{n}(t) \cdot \big(\mathbf{p} - \mathbf{x}(t)\big) &=& 0, \\ \mathbf{b}(t) \cdot \big(\mathbf{p} - \mathbf{x}(t)\big) &=& 0, \end{array} \tag{26}$$

respectively, where $(\mathbf{t}, \mathbf{n}, \mathbf{b})$ is the Frenet frame (11). The Frenet-Serret equations describing the variation of the Frenet frame read

$$\begin{pmatrix} \mathbf{t}' \\ \mathbf{n}' \\ \mathbf{b}' \end{pmatrix} = \sigma \begin{pmatrix} 0 & \kappa & 0 \\ -\kappa & 0 & \tau \\ 0 & -\tau & 0 \end{pmatrix} \begin{pmatrix} \mathbf{t} \\ \mathbf{n} \\ \mathbf{b} \end{pmatrix}, \tag{27}$$

where σ is the speed, κ is the curvature, and τ is the torsion of $\mathbf{x}(t)$.

The equation of the osculating plane in (26) has the form

$$f(t) = \mathbf{b}(t) \cdot \mathbf{p}, \tag{28}$$

where we define $f(t) := \mathbf{b}(t) \cdot \mathbf{x}(t)$. For a unit vector field $\mathbf{b}(t)$, the function $f(t)$ expresses the distance of the corresponding osculating plane from the origin.

It can be proved that (under some natural assumptions) differentiating (28) and using (27) gives an equation of the rectifying plane. Differentiating again yields an equation of the normal plane. It follows that starting from a given rational unit vector $\mathbf{b}(t)$ and a given rational function $f(t)$, the points of a spatial curve $\mathbf{x}(t)$ may be identified as the intersection points of the associated osculating, rectifying and normal planes.

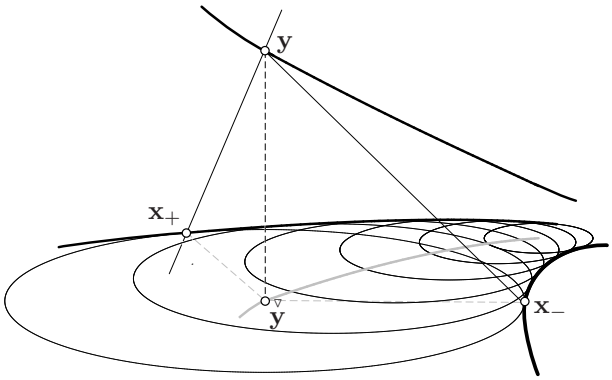

Figure 5: An MPH curve $\mathbf{y} \subset \mathbb{R}^{2,1}$ with its orthogonal projection $\overset{\triangledown}{\mathbf{y}} \subset \mathbb{R}^2$ and the associated PH curves $\mathbf{x}_\pm \subset \mathbb{R}^2$.

However, $\mathbf{x}(t)$ is not rational in general since the normalised tangent and normal vectors contain square root terms. To resolve this issue, the authors of [47] consider a modified *rational* system of three planes instead, namely

$$\mathbf{b}(t) \cdot \mathbf{p} = f(t), \quad \mathbf{b}'(t) \cdot \mathbf{p} = f'(t), \quad \mathbf{b}''(t) \cdot \mathbf{p} = f''(t). \tag{29}$$

The first plane is still the osculating plane, but the other two are not the rectifying and normal planes any more (as $\mathbf{b}'(t)$ is generally not unit and $\mathbf{b}''(t)$ is not orthogonal to $\mathbf{b}'(t)$).

Modifying the system of planes (26) to (29) does not change the main contribution of the introduced approach: one can construct a curve with a given (not necessarily unit) binormal vector field. With a slight alteration, system (29) can be used for constructing rational spatial PH curves: instead of $\mathbf{b}(t)$, the authors of [47] prescribe a rational unit vector field $\mathbf{t}(t)$ tangent to the sought-after curve $\mathbf{x}(t)$ and hence guarantee its PH character. The vector $\mathbf{b}(t)$ is computed subsequently.

It is proved in [47] that all spatial rational PH curves can be expressed in the form

$$(\mathbf{u}(t) \cdot [\mathbf{u}'(t) \times \mathbf{u}''(t)])\mathbf{x}(t) = f(t)\mathbf{u}'(t) \times \mathbf{u}''(t) + f'(t)\mathbf{u}''(t) \times \mathbf{u}(t) + f''(t)\mathbf{u}(t) \times \mathbf{u}'(t), \tag{30}$$

where $\mathbf{u}(t) = \mathbf{t}(t) \times \mathbf{t}'(t)$ (in general not a unit binormal vector) and

$$\mathbf{t}(t) = \frac{\big(2a(t), 2b(t), 1 - a^2(t) - b^2(t)\big)^\top}{1 + a^2(t) + b^2(t)} \tag{31}$$

for any two rational functions $a(t), b(t) \in \mathbb{R}(t)$. However, it still remains an open problem how to choose $a(t), b(t), f(t)$ in (30) and (31) in order to obtain all *polynomial* PH curves from the formula for rational PH curves (as a space analogy to the result from [42]).

In addition, all spatial rational PH curves are in fact obtained as the edges of regression of developable surfaces regarded as the envelopes of a 1-parameter family of (osculating) planes (28). A further insight into rational spatial PH curves is provided in [70] using their dual representation.

4.2 Rational Minkowski spatial PH curves

As discussed before, if $\mathrm{MAT}(\Omega)$ is an MPH curve $\mathbf{y}$, then the boundary curves $\mathbf{x}_\pm$ of Ω associated with $\mathbf{y}$ and all offsets of the boundary (see Fig. 5) are (piece-wise) rational, cf. (19). We rewrite (19) in the form

$$\mathbf{x}_\pm = \overset{\triangledown}{\mathbf{y}} - y_3 \mathbf{n}_\pm, \tag{32}$$

where

$$\mathbf{n}_\pm = \frac{1}{\varrho^2 + y_3'^2} \begin{pmatrix} y_3' y_1' \mp \varrho y_2' \\ y_3' y_2' \pm \varrho y_1' \end{pmatrix}. \tag{33}$$

It can be shown by a direct computation that $\mathbf{n}_\pm$ is a unit vector perpendicular to $\mathbf{x}_\pm$. Moreover, $\mathbf{n}_\pm$ is rational if and only if ϱ is rational. Hence, for any MPH curve $\mathbf{y} \subset \mathbb{R}^{2,1}$, the associated curves $\mathbf{x}_\pm \subset \mathbb{R}^2$ possess a normal vector field rationally parametrising the unit circle, i.e., $\mathbf{x}_\pm$ are rational PH curves.

This observation is closely related to the result of [67], which states that any rational MPH curve $\mathbf{y}$ in $\mathbb{R}^{2,1}$ can be constructed starting from an (associated) planar rational PH curve $\mathbf{x}$ in $\mathbb{R}^2$ and a rational function r in the form

$$\mathbf{y}(t) = (x_1 + rn_1, x_2 + rn_2, r)^\top = \overset{\triangle}{\mathbf{x}}(t) + r(t)\tilde{\mathbf{n}}(t), \tag{34}$$

with $\overset{\triangle}{\mathbf{x}} = (x_1, x_2, 0)^\top$ (read $\overset{\triangle}{\mathbf{x}}$ as '$\mathbf{x}$ up') and $\tilde{\mathbf{n}} = (n_1, n_2, 1)^\top$, where $\mathbf{n} = (n_1, n_2)^\top = \mathbf{x}'^{\perp}/\sigma$. Using (34), one can obtain an expression for all rational MPH curves; see formula (30) in [67].

We would like to recall that the paper [47], primarily devoted to Euclidean rational PH curves, contains a general result (see [47, Proposition 2]) which is then applied also to MPH curves (see [47, Proposition 3]). It is enough to take the vector $\mathbf{t}$, cf. (31), in the form

$$\mathbf{t}(t) = \frac{\big(1 - a^2(t) + b^2(t), 2a(t), 2b(t),\big)^\top}{1 + a^2(t) - b^2(t)}. \tag{35}$$

We end the section with an example which reveals an interesting close analogy between spatial rational PH curves in Euclidean and Minkowski space. We believe that the following construction may help to motivate further study in this field.

Example 4.1 *Consider the spatial rational PH curve given by the PH parametrisation*

$$\mathbf{y}(t) = \left(\frac{3t^4 - 4t^2 + 12}{4t^2}, \frac{3t^4 + 4}{2t^3}, \frac{t^4 + 12}{4t}\right)^\top.$$

Consider a family of all circles with midpoints on the curve $\overset{\triangledown}{\mathbf{y}} = (y_1, y_2)^\top$

$$\overset{\triangledown}{\mathbf{y}}(t) = \left(\frac{3t^4 - 4t^2 + 12}{4t^2}, \frac{3t^4 + 4}{2t^3}\right)^\top$$

and with the corresponding, now imaginary, *radii*

$$r(t) = y_3(t)\,\mathrm{i} = \frac{t^4 + 12}{4t}\mathrm{i},$$

where $\mathrm{i} = \sqrt{-1}$. *Using imaginary radii enables us to use Euclidean inner product for expressing an equation of a circle (analogously to the Minkowski case). We consider the domain* Ω *whose boundary is the envelope of the 1-parameter family of imaginary circles*

$$\|\mathbf{x} - \overset{\triangledown}{\mathbf{y}}(t)\|^2 + y_3^2(t) = \|\mathbf{x} - \overset{\triangledown}{\mathbf{y}}(t)\|^2 - (y_3(t)\,\mathrm{i})^2 = 0.$$

It can be shown that the corresponding boundary curves $\mathbf{x}_\pm$ *associated with* $\mathbf{y}$ *are again rational PH curves, this time in* $\mathbb{C}(t)$. *In particular, we obtain*

$$\mathbf{x}_+ = \left(\frac{(t^2+2)(t^5+2t^4\mathrm{i}+2t^3+2t^2\mathrm{i}+12\mathrm{i})}{8t^2(t+\mathrm{i})^2}, -\frac{\mathrm{i}(t^2+2)(t^6+2t^5\mathrm{i}-2t^4+8t^3\mathrm{i}+4t^2+8t\mathrm{i}-8)}{8t^3(t+\mathrm{i})^2}\right)^\top,$$

$$\mathbf{x}_- = \left(\frac{(t^2+2)(-t^5+2t^4\mathrm{i}-2t^3+2t^2\mathrm{i}+12\mathrm{i})}{8t^2(-t+\mathrm{i})^2}, \frac{\mathrm{i}(t^2+2)(-t^6+2t^5\mathrm{i}+2t^4+8t^3\mathrm{i}-4t^2+8t\mathrm{i}+8)}{8t^3(-t+\mathrm{i})^2}\right)^\top$$

with the corresponding squared parameter speeds

$$\mu_+^2 = \frac{(-4t^7 + 3t^6\mathrm{i} - 6t^5 + 6t^4\mathrm{i} - 12t^2\mathrm{i} + 24t - 24\mathrm{i})^2}{16(-t+\mathrm{i})^2 t^8},$$

$$\mu_-^2 = \frac{(4t^7 + 3t^6\mathrm{i} + 6t^5 + 6t^4\mathrm{i} - 12t^2\mathrm{i} - 24t - 24\mathrm{i})^2}{16(t+\mathrm{i})^2 t^8}.$$

The above consideration brings us to the idea to construct all rational (Euclidean) PH curves by the method which was originally used for MPH curves. Analogously to the construction of MPH curves in $\mathbb{R}^{2,1}$, *rational spatial PH curves can be obtained if we prescribe a special (complex) rational planar PH curve and a rational function* $r(t) \in \mathbb{C}(t)$. *Hence, using* (5) *we arrive at*

$$\mathbf{y} = \frac{1}{2(k^2+l^2)(kl' - k'l)} \begin{pmatrix} 2(ll' - kk')g + (k^2 - l^2)g' \\ 2(k'l + kl')g - 2klg' \\ 0 \end{pmatrix} + \frac{\mathrm{i}r}{k^2+l^2} \begin{pmatrix} 2kl \\ k^2 - l^2 \\ k^2 + l^2 \end{pmatrix}. \tag{36}$$

Similarly to the MPH case, cf. [67], (36) *gives all 'complex' PH curves in* $\mathbb{C}^3$. *However, it is not yet known how to identify suitable tuples of* $k(t), l(t) \in \mathbb{C}[t]$ *and* $g(t), r(t) \in \mathbb{C}(t)$ *for* (36) *to yield only* real *PH curves in* $\mathbb{R}^3$.

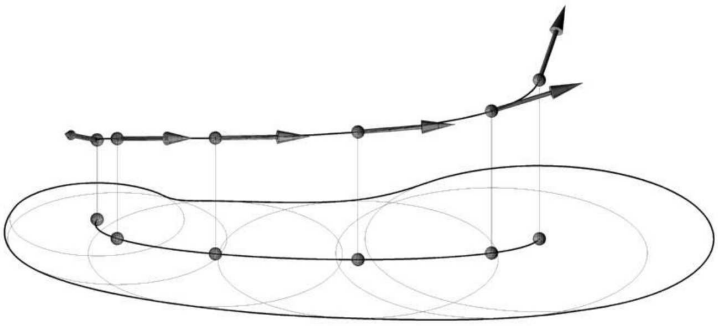

Figure 6: MPH Hermite interpolation: Hermite data are sampled from the MAT of a given domain and each segment is replaced by an MPH interpolant. This in turn gives a PH approximation of the boundary and all its offsets.

5 Interpolation techniques with PH curves

Generating valid tool paths in NURBS form has become a universal standard in technical applications such as CNC machining in recent years. Hence, shape offsets and corresponding algorithms have been widely studied in Computer-Aided Design and Manufacturing, see e.g. [77] and references therein for more details. However, free-form NURBS shapes do not possess rational offsets in general and thus suitable approximation techniques are required.

The approximate techniques for offsets are now widely used in CAD systems since they are capable of dealing with problems appearing in technical practice mentioned above – but usually at the expense of great computational effort. Therefore, it is worthwhile to investigate exact techniques based on shapes with the Pythagorean property (e.g. PH curves) yielding the exact rational offsets. Compared to classical approximation techniques, not offsets but the base shape is approximated and it is guaranteed that all corresponding offsets are rational. Therefore, only one approximation step is required even if more than one offset is needed. Moreover, all the offsets are at an exact constant distance from each other.

In the case of polynomial PH curves we can exploit their polynomial parametric speed. Hence, the interpolation/approximation techniques based on polynomial PH curves are used when formulating exact real time interpolator algorithms for CNC machines; see [46, 96, 23]

In this section, we list and classify several (M)PH interpolation techniques which form the cornerstone of subsequent approximation algorithms formulated for particular problems originating in technical practice; see Fig. 6.

5.1 Interpolation in Euclidean plane and space

Table 1 summarises known results on classical Hermite interpolation in the Euclidean plane and space.

Other types of planar algorithms include

- PH interpolation by various types of spirals [104, 34, 103, 50, 49],
- PH interpolation using the homotopy method [4],
- geometric Lagrange interpolation by PH curves [56, 57],
- PH interpolation with shape control [51], via control polygons [84],
- interpolation via double (two arcs of) PH curves [30, 8],
- rational PH interpolation [89, 99],
- and other methods [62, 20, 52].

An important theoretical result on PH approximation was presented in [21].

In the case of spatial curves, we can distinguish the following methods:

Table 1: Hermite interpolation by Euclidean PH curves of degree $\mathbf{d}$; $\mathbb{H}$ is the field of quaterninons and a stands for approximation order.

data	d	solutions	results	ref.
Hermite interpolation in $\mathbb{R}^2$				
G^1	3	2 (quadratic eq.)	One of the solutions has $a = 4$ at generic points. Conditions on interpolants without a loop are known.	[79, 64, 11, 97]
C^1	5	4 (quadratic eqs.)	The best solution can be identified via its rotation index or a topological criterion.	[29, 83, 17]
G^2	7	8 (quartic eqs.)	One of the solutions has $a = 6$ at generic points. Inflections reduce a.	[58]
C^2	9	4 (quadratic eqs.)	One of the solutions has $a = 6$ at all points.	[27, 100]
Hermite interpolation in $\mathbb{R}^3$				
G^1	3	2 (quadratic eq.)	One of the solutions has $a = 4$ at generic points.	[59, 78, 74]
C^1	5	2-parameter system (quadratic eqs. in $\mathbb{H}$)	One solution has the best $a = 4$, preserves planarity and symmetry.	[36, 101, 37]
C^2	9	4-parameter system (quadratic eqs. in $\mathbb{H}$)	One solution has the best $a = 6$, preserves planarity and symmetry.	[28, 102]

- PH interpolation by helical curves [54, 55],
- an evolution based framework [2].

Further results on PH quintic interpolation can be found in [94].

Of special importance are the G^1 and G^2 interpolation methods developed in [47], where spatial rational PH curves are employed. The resulting degree of the interpolant depends on the choice of tangent indicatrix and an extra polynomial/rational function.

5.2 Interpolation in Minkowski plane and space

Similarly to the Euclidean case, Table 2 reports Hermite interpolation algorithms in the Minkowski plane and space.

We remark that some of the solutions of the G^1 problem investigated in [64] do not preserve the orientation of the input data. Asymptotically, only 2 of the 4 solutions match the orientation. Moreover, we emphasise that the results on Hermite interpolation in $\mathbb{R}^{2,1}$ [64, 66, 69] cover not only interpolation in $\mathbb{R}^{1,1}$ (or any time-like plane in $\mathbb{R}^{2,1}$ in general), but also in $\mathbb{R}^2$ (a special space-like plane); cf. Table 1.

6 Conclusion

In this brief survey of recent results in the field of PH and MPH curves, we summarised the main ideas that have shaped its development in the last years. A literature survey on PH curves up to 2008 was carried out by Farouki in [24]. The objective of this paper was to overview the literature which is not included in the aforementioned book. The article focused on three active areas of research on PH curves: polynomial PH curves, rational PH curves, and interpolation by PH curves in Euclidean and Minkowski plane and space.

We conclude the paper by a list of open problems, which may steer future development in the field of PH curves.

- Generalise the class of double PH curves (and potentially other properties such as RRMFs) to Minkowski space.
- The most important PH interpolation problems seem to have been solved satisfactorily. However, there is scope for investigation of motion design applications, c.f. [71].
- PN curves: curves on polynomial or rational (non-PN) surfaces such that their corresponding offset curves w.r.t. the surface are rational.

Table 2: Hermite interpolation by Minkowski PH curves of degree $\mathbf{d}$; $\mathcal{C}\ell(2,1)$ is the Clifford algebra associated with $\mathbb{R}^{2,1}$ and a stands for approximation order.

data	d	solutions	results	ref.
Hermite interpolation in $\mathbb{R}^{1,1}$				
G^1	3	4 (2 quadratic eqs.)	One of the solutions has $a = 4$ at generic points.	[64]
C^1	5	16 (quadratic eqns. in $\mathcal{C}\ell(2,1)$)	One of the solutions has $a = 4$ at generic points.	[66]
C^2	9	16 (quadratic and lin. eqs. in $\mathcal{C}\ell(2,1)$)	One of the solutions has $a = 6$.	[69]
Hermite interpolation in $\mathbb{R}^{2,1}$				
G^1	3	4 (2 quadratic eqs.)	One of the solutions has $a = 4$ at generic points.	[64]
G^1	4	8 (quadratic eqs.)	Also extended to $C^{1/2}$ and two-step C^1.	[60]
G^1	5	1 (lin. equation)	The solution has $a = 4$ at generic points.	[68]
C^1	5	sixteen 2-parameter systems (quadratic eqs. in $\mathcal{C}\ell(2,1)$)	One solution has the best $a = 4$, preserves planarity and symmetry of the data.	[66]
C^2	9	sixteen 4-parameter systems (quadr. and lin. eqs. in $\mathcal{C}\ell(2,1)$)	One solution has the best $a = 6$, preserves planarity and symmetry of the data.	[69]

- Study of 'almost-PH curves', i.e., of curves satisfying the PH condition (2) only approximately: $x_1'(t)^2 + x_2'(t)^2 \simeq \sigma(t)^2$ with a given error tolerance.
- Identification of (complex) planar PH curves yielding real spatial PH curves, c.f. Example 4.1.
- Problems regarding interpolation by PN and MOS surfaces, as an analogy of the close relationship between PH and MPH curves, have not been explored yet.

Acknowledgments

The first author thanks EPSRC for supporting this work through grant EP/H030115/1. The second author was supported by the European Regional Development Fund (ERDF), project "NTIS - New Technologies for Information Society", European Centre of Excellence, CZ.1.05/1.1.00/02.0090.

References

[1] AICHHOLZER, O., AIGNER, W., AURENHAMMER, F., HACKL, T., JÜTTLER, B., AND RABL, M. Medial axis computation for planar free-form shapes. *Computer-Aided Design 41*, 5 (2009), 339–349.

[2] AIGNER, M., ŠÍR, Z., AND JÜTTLER, B. Evolution-based least-squares fitting using Pythagorean hodograph spline curves. *Computer Aided Geometric Design 24*, 6 (2007), 310–322. 4th International Conference on Geometric Modeling and Processing (GMP 2006).

[3] AIT-HADDOU, R., HERZOG, W., AND BIARD, L. Pythagorean-hodograph ovals of constant width. *Computer Aided Geometric Design 25*, 4-5 (2008), 258–273. Pythagorean-Hodograph Curves and Related Topics.

[4] ALBRECHT, G., AND FAROUKI, R. Construction of C^2 Pythagorean-hodograph interpolating splines by the homotopy method. *Advances in Computational Mathematics 5* (1996), 417–442.

[5] ALTMANN, S. L. *Rotations, quaternions, and double groups*. Dover Publications, 2005.

[6] BASTL, B., JÜTTLER, B., KOSINKA, J., AND LÁVIČKA, M. Volumes with piecewise quadratic medial surface transforms: Computation of boundaries and trimmed offsets. *Computer-Aided Design 42*, 6 (2010), 571–579.

[7] BASTL, B., KOSINKA, J., AND LÁVIČKA, M. A symbolic-numerical envelope algorithm using quadratic MOS patches. In *SPM '09: 2009 SIAM/ACM Joint Conference on Geometric and Physical Modeling* (New York, NY, USA, 2009), ACM, pp. 175–186.

[8] BASTL, B., SLABÁ, K., AND BYRTUS, M. Planar Hermite interpolation with uniform and non-uniform TC-biarcs. *Computer Aided Geometric Design 30*, 1 (2013), 58 – 77. Recent Advances in Applied Geometry.

[9] BELTRAN, J. V., AND MONTERDE, J. A characterization of quintic helices. *J. Comput. Appl. Math. 206*, 1 (Sept. 2007), 116–121.

[10] BLUM, H. A transformation for extracting new descriptors of shape. In *Models for the perception of speech and visual form*, W. Wathen-Dunn, Ed. MIT Press, 1967, pp. 362–380.

[11] BYRTUS, M., AND BASTL, B. G^1 Hermite interpolation by PH cubics revisited. *Computer Aided Geometric Design 27* (November 2010), 622–630.

[12] CAO, L., JIA, Z., AND LIU:, J. Computation of medial axis and offset curves of curved boundaries in planar domains based on the Cesaro's approach. *Computer Aided Geometric Design 26*, 4 (2009), 444–454.

[13] CAO, L., AND LIU, J. Computation of medial axis and offset curves of curved boundaries in planar domain. *Computer-Aided Design 40* (2008), 465–475.

[14] CHO, H., CHOI, H., KWON, S.-H., LEE, D., AND WEE, N.-S. Clifford algebra, Lorentzian geometry and rational parametrization of canal surfaces. *Computer Aided Geometric Design 21* (2004), 327–339.

[15] CHOI, H., CHOI, S., AND MOON:, H. Mathematical theory of medial axis transform. *Pacific Journal of Mathematics 181* (1997), 57–88.

[16] CHOI, H., LEE, D., AND MOON, H. Clifford algebra, spin representation and rational parameterization of curves and surfaces. *Advances in Computational Mathematics 17* (2002), 5–48.

[17] CHOI, H. I., FAROUKI, R. T., KWON, S.-H., AND MOON, H. P. Topological criterion for selection of quintic Pythagorean-hodograph hermite interpolants. *Computer Aided Geometric Design 25*, 6 (2008), 411–433.

[18] CHOI, H. I., AND HAN, C. Y. Euler-Rodrigues frames on spatial Pythagorean-hodograph curves. *Computer Aided Geometric Design 19*, 8 (2002), 603–620.

[19] CHOI, H. I., HAN, C. Y., MOON, H. P., ROH, K. H., AND WEE, N.-S. Medial axis transform and offset curves by Minkowski Pythagorean hodograph curves. *Computer-Aided Design 31*, 1 (Jan. 1999), 59–72.

[20] CHOI, H. I., AND KWON, S.-H. Absolute hodograph winding number and planar PH quintic splines. *Computer Aided Geometric Design 25*, 4-5 (2008), 230–246. Pythagorean-Hodograph Curves and Related Topics.

[21] CHOI, H. I., AND MOON, H. P. Weierstrass-type approximation theorems with Pythagorean hodograph curves. *Computer Aided Geometric Design 25*, 4-5 (2008), 305–319. Pythagorean-Hodograph Curves and Related Topics.

[22] DIETZ, R., HOSCHEK, J., AND JÜTTLER, B. An algebraic approach to curves and surfaces on the sphere and on other quadrics. *Computer Aided Geometric Design 10*, 3-4 (1993), 211–229.

[23] FARIN, G., HOSCHEK, J., AND KIM, M.-S., Eds. *Handbook of Computer Aided Geometric Design*. Elsevier, 2002.

[24] FAROUKI, R. *Pythagorean-Hodograph Curves: Algebra and Geometry Inseparable*. Springer, 2008.

[25] FAROUKI, R., DOSPRA, P., AND SAKKALIS, T. Scalar-vector algorithm for the roots of quadratic quaternion polynomials, and the characterization of quintic rational rotation-minimizing frame curves. *Journal of Symbolic Computation 58* (2013), 1–17.

[26] FAROUKI, R., GIANNELLI, C., SAMPOLI, M., AND SESTINI, A. Rotation-minimizing osculating frames. *Computer Aided Geometric Design* (2013). Article in Press.

[27] FAROUKI, R., MANJUNATHAIAH, J., AND JEE, S. Design of rational CAM profiles with Pythagorean-hodograph curves. *Mechanism and Machine Theory 33*, 6 (1998), 669–682.

[28] FAROUKI, R., MANNI, C., AND SESTINI, A. Spatial C^2 PH quintic splines. In *Curve and Surface Design: St. Malo 2002*, T. Lyche, M. Mazure, and L. Schumaker, Eds. Nashboro Press, 2003, pp. 147–156.

[29] FAROUKI, R., AND NEFF, C. Hermite interpolation by Pythagorean-hodograph quintics. *Mathematics of Computation 64*, 212 (1995), 1589–1609.

[30] FAROUKI, R., AND PETERS, J. Smooth curve design with double-Tschirnhausen cubics. *Annals of Numerical Mathematics 3* (1996), 63–82.

[31] FAROUKI, R., AND SAKKALIS, T. Pythagorean hodographs. *IBM Journal of Research and Development 34*, 5 (1990), 736–752.

[32] FAROUKI, R., AND SAKKALIS, T. Pythagorean-hodograph space curves. *Adv. Comput. Math. 2* (1994), 41–66.

[33] FAROUKI, R., AND SAKKALIS, T. Rational space curves are not "unit speed". *Computer Aided Geometric Design 24* (2007), 238–240.

[34] FAROUKI, R. T. Pythagorean-hodograph quintic transition curves of monotone curvature. *Computer-Aided Design 29*, 9 (1997), 601–606.

[35] FAROUKI, R. T. Quaternion and Hopf map characterizations for the existence of rational rotation-minimizing frames on quintic space curves. *Adv. Comput. Math. 33* (October 2010), 331–348.

[36] FAROUKI, R. T., AL KANDARI, M., AND SAKKALIS, T. Hermite interpolation by rotation-invariant spatial Pythagorean-hodograph curves. *Advances in Computational Mathematics 17* (2002), 369–383.

[37] FAROUKI, R. T., GIANNELLI, C., MANNI, C., AND SESTINI, A. Identification of spatial PH quintic Hermite interpolants with near-optimal shape measures. *Computer Aided Geometric Design 25*, 4-5 (2008), 274–297. Pythagorean-Hodograph Curves and Related Topics.

[38] FAROUKI, R. T., GIANNELLI, C., MANNI, C., AND SESTINI, A. Quintic space curves with rational rotation-minimizing frames. *Computer Aided Geometric Design 26*, 5 (2009), 580–592.

[39] FAROUKI, R. T., GIANNELLI, C., AND SESTINI, A. Helical polynomial curves and double Pythagorean hodographs I. Quaternion and hopf map representations. *Journal of Symbolic Computation 44*, 2 (2009), 161–179.

[40] FAROUKI, R. T., GIANNELLI, C., AND SESTINI, A. Helical polynomial curves and double Pythagorean hodographs II. Enumeration of low-degree curves. *Journal of Symbolic Computation 44*, 4 (2009), 307–332.

[41] FAROUKI, R. T., HAN, C. Y., MANNI, C., AND SESTINI, A. Characterization and construction of helical polynomial space curves. *J. Comput. Appl. Math. 162*, 2 (Jan. 2004), 365–392.

[42] FAROUKI, R. T., AND POTTMANN, H. Polynomial and rational Pythagorean-hodograph curves reconciled. In *Proceedings of the 6th IMA Conference on the Mathematics of Surfaces* (New York, NY, USA, 1996), Clarendon Press, pp. 355–378.

[43] FAROUKI, R. T., AND SAKKALIS, T. Rational rotation-minimizing frames on polynomial space curves of arbitrary degree. *Journal of Symbolic Computation 45*, 8 (2010), 844–856.

[44] FAROUKI, R. T., AND SAKKALIS, T. Equivalence of distinct characterizations for rational rotation-minimizing frames on quintic space curves. *Computer Aided Geometric Design 28*, 7 (2011), 436–445.

[45] FAROUKI, R. T., AND SAKKALIS, T. A complete classification of quintic space curves with rational rotation-minimizing frames. *Journal of Symbolic Computation 47*, 2 (2012), 214–226.

[46] FAROUKI, R. T., AND TSAI, Y.-F. Exact taylor series coefficients for variable-feedrate CNC curve interpolators. *Computer-Aided Design 33*, 2 (2001), 155–165.

[47] FAROUKI, R. T., AND ŠÍR, Z. Rational Pythagorean-hodograph space curves. *Computer Aided Geometric Design 28* (February 2011), 75–88.

[48] FAROUKI, T. R., GIANNELLI, CARLOTTA AMD MANNI, C., AND SESTINI, A. Design of rational rotation-minimizing rigid borotation-minimizing osculating framesrotation-minimizing osculating framesdy motions by hermite interpolation. *Math. Comput. 81*, 278 (2012), 879–903.

[49] GOODMAN, T., MEEK, D., AND WALTON, D. An involute spiral that matches Hermite data in the plane. *Computer Aided Geometric Design 26*, 7 (2009), 733–756.

[50] HABIB, Z., AND SAKAI, M. On ph quintic spirals joining two circles with one circle inside the other. *Computer-Aided Design 39*, 2 (2007), 125–132.

[51] HABIB, Z., AND SAKAI, M. Pythagorean hodograph quintic transition between two circles with shape control. *Computer Aided Geometric Design 24*, 5 (2007), 252–266.

[52] HABIB, Z., AND SAKAI, M. Transition between concentric or tangent circles with a single segment of PH quintic curve. *Computer Aided Geometric Design 25*, 4-5 (2008), 247–257. Pythagorean-Hodograph Curves and Related Topics.

[53] HAN, C. Y. Nonexistence of rational rotation-minimizing frames on cubic curves. *Computer Aided Geometric Design 25*, 4-5 (2008), 298–304. Pythagorean-Hodograph Curves and Related Topics.

[54] HAN, C. Y. Geometric hermite interpolation by monotone helical quintics. *Computer Aided Geometric Design 27*, 9 (2010), 713–719.

[55] HAN, C. Y., AND KWON, S.-H. Cubic helical splines with Frenet-frame continuity. *Computer Aided Geometric Design 28*, 7 (2011), 395–406.

[56] JAKLIČ, G., KOZAK, J., KRAJNC, M., VITRIH, V., AND ŽAGAR, E. Geometric Lagrange interpolation by planar cubic Pythagorean-hodograph curves. *Comput. Aided Geom. Des. 25*, 9 (2008), 720–728.

[57] JAKLIČ, G., KOZAK, J., KRAJNC, M., VITRIH, V., AND ŽAGAR, E. An approach to geometric interpolation by Pythagorean-hodograph curves. *Advances in Computational Mathematics 37* (2012), 123–150.

[58] JÜTTLER, B. Hermite interpolation by Pythagorean hodograph curves of degree seven. *Math. Comp. 70* (2001), 1089–1111.

[59] JÜTTLER, B., AND MÄURER, C. Cubic Pythagorean hodograph spline curves and applications to sweep surface modeling. *Computer-Aided Design 31*, 1 (1999), 73–83.

[60] KIM, G.-I., AND AHN, M.-H. C^1 Hermite interpolation using MPH quartic. *Computer Aided Geometric Design 20* (2003), 469–492.

[61] KIM, G.-I., AND LEE, S. Pythagorean-hodograph preserving mappings. *J. Comput. Appl. Math. 216*, 1 (2008), 217–226.

[62] KONG, J. H., JEONG, S. P., LEE, S., AND KIM, G. I. C^1 Hermite interpolation with simple planar PH curves by speed reparametrization. *Computer Aided Geometric Design 25*, 4-5 (2008), 214–229. Pythagorean-Hodograph Curves and Related Topics.

[63] KOSINKA, J., AND JÜTTLER, B. Cubic helices in Minkowski space. *Sitzungsber. Österr. Akad. Wiss., Abt. II 215* (2006), 13–35.

[64] KOSINKA, J., AND JÜTTLER, B. G^1 Hermite interpolation by Minkowski Pythagorean hodograph cubics. *Computer Aided Geometric Design 23* (2006), 401–418.

[65] KOSINKA, J., AND JÜTTLER, B. MOS surfaces: Medial surface transforms with rational domain boundaries. In *The Mathematics of Surfaces XII*, vol. 4647 of *Lecture Notes in Computer Science*. Springer, 2007, pp. 245–262.

[66] KOSINKA, J., AND JÜTTLER, B. C^1 Hermite interpolation by Pythagorean hodograph quintics in Minkowski space. *Advances in Computational Mathematics 30* (2009), 123–140.

[67] KOSINKA, J., AND LÁVIČKA, M. On rational Minkowski Pythagorean hodograph curves. *Computer Aided Geometric Design 27*, 7 (2010), 514–524.

[68] KOSINKA, J., AND LÁVIČKA, M. A unified Pythagorean hodograph approach to medial axis transform and offset approximation. *Journal of Computational and Applied Mathematics 235*, 12 (2011), 3413–3424.

[69] KOSINKA, J., AND ŠÍR, Z. C^2 Hermite interpolation by Minkowski Pythagorean hodograph curves and medial axis transform approximation. *Computer Aided Geometric Design 27*, 8 (November 2010), 631–643.

[70] KOZAK, J., KRAJNC, M., AND VITRIH, V. Dual representation of spatial rational pythagorean-hodograph curves. *Computer Aided Geometric Design* (2013). Article in Press.

[71] KRAJNC, M., AND VITRIH, V. Motion design with Euler-Rodrigues frames of quintic Pythagorean-hodograph curves. *Mathematics and Computers in Simulation 82*, 9 (2012), 1696–1711.

[72] KRASAUSKAS, R. Branching blend of natural quadrics based on surfaces with rational offsets. *Computer Aided Geometric Design 25* (2008), 332–341.

[73] KUBOTA, K. Pythagorean triples in unique factorization domains. *American Mathematical Monthly 79* (1972), 503–505.

[74] KWON, S.-H. Solvability of Hermite interpolation by spatial Pythagorean-hodograph cubics and its selection scheme. *Computer Aided Geometric Design 27*, 2 (2010), 138–149.

[75] LÁVIČKA, M., AND BASTL, B. PN surfaces and their convolutions with rational surfaces. *Computer Aided Geometric Design 25* (2008), 763–774.

[76] LÁVIČKA, M., AND VRŠEK, J. On a special class of polynomial surfaces with Pythagorean normal vector fields. In *Curves and Surfaces* (2012), J.-D. Boissonnat, P. Chenin, A. Cohen, C. Gout, T. Lyche, M.-L. Mazure, and L. Schumaker, Eds., vol. 6920 of *Lecture Notes in Computer Science*, Springer Berlin Heidelberg, pp. 431–444.

[77] MAEKAWA, T. An overview of offset curves and surfaces. *Computer-Aided Design 31* (1999), 165–173.

[78] MÄURER, C., AND JÜTTLER, B. Rational approximation of rotation minimizing frames using Pythagorean-hodograph cubics. *J. GEOM. GRAPHICS 3*, 2 (1999), 141–159.

[79] MEEK, D. S., AND WALTON, D. J. Geometric Hermite interpolation with Tschirnhausen cubics. *J. Comput. Appl. Math. 81*, 2 (1997), 299–309.

[80] MOETAKEF IMANI, B., AND GHANDEHARIUN, A. Real-time PH-based interpolation algorithm for high speed CNC machining. *The International Journal of Advanced Manufacturing Technology 56*, 5-8 (2011), 619–629.

[81] MONTERDE, J., AND ONGAY, F. An isoperimetric type problem for primitive pythagorean hodograph curves. *Computer Aided Geometric Design 29*, 8 (2012), 626–647.

[82] MOON, H. Minkowski Pythagorean hodographs. *Computer Aided Geometric Design 16* (1999), 739–753.

[83] MOON, H. P., FAROUKI, R. T., AND CHOI, H. I. Construction and shape analysis of PH quintic Hermite interpolants. *Computer Aided Geometric Design 18*, 2 (2001), 93–115.

[84] PELOSI, F., SAMPOLI, M., FAROUKI, R., AND MANNI, C. A control polygon scheme for design of planar C^2 PH quintic spline curves. *Computer Aided Geometric Design 24* (2007), 28–52.

[85] PETERNELL, M. Rational two-parameter families of spheres and rational offset surfaces. *Journal of Symbolic Computation 45*, 1 (2010), 1–18.

[86] PETERNELL, M., AND ODEHNAL, B. On generalized LN-surfaces in 4-space. In *Proceedings of 'ISSAC08'* (2008), pp. 223–230.

[87] PETERNELL, M., ODEHNAL, B., AND SAMPOLI, M. On quadratic two-parameter families of spheres and their envelopes. *Computer Aided Geometric Design 25* (2008), 342–355.

[88] PETERNELL, M., AND POTTMANN, H. A Laguerre geometric approach to rational offsets. *Computer Aided Geometric Design 15* (1998), 223–249.

[89] POTTMANN, H. Curve design with rational Pythagorean-hodograph curves. *Advances in Computational Mathematics 3* (1995), 147–170.

[90] POTTMANN, H. Rational curves and surfaces with rational offsets. *Computer Aided Geometric Design 12*, 2 (1995), 175–192.

[91] POTTMANN, H., AND PETERNELL, M. Applications of Laguerre geometry in CAGD. *Computer Aided Geometric Design 15* (1998), 165–186.

[92] SAKKALIS, T., AND FAROUKI, R. T. Pythagorean-hodograph curves in Euclidean spaces of dimension greater than 3. *Journal of Computational and Applied Mathematics 236*, 17 (2012), 4375–4382.

[93] SAKKALIS, T., FAROUKI, R. T., AND VASERSTEIN, L. Non-existence of rational arc length parameterizations for curves in R^n. *Journal of Computational and Applied Mathematics 228*, 1 (2009), 494–497.

[94] SESTINI, A., LANDOLFI, L., AND MANNI, C. On the approximation order of a space data-dependent PH quintic Hermite interpolation scheme. *Computer Aided Geometric Design 30*, 1 (2012), 148–158.

[95] SHAFAREVICH, I. R. *Basic algebraic geometry*. Springer Verlag, 1974.

[96] TSAI, Y.-F., FAROUKI, R. T., AND FELDMAN, B. Performance analysis of CNC interpolators for time-dependent feedrates along PH curves. *Computer Aided Geometric Design 18*, 3 (2001), 245–265.

[97] ČERNOHORSKÁ, E., AND ŠÍR, Z. Support function of Pythagorean hodograph cubics and G^1 Hermite interpolation. In *Advances in Geometric Modeling and Processing*, B. Mourrain, S. Schaefer, and G. Xu, Eds., vol. 6130 of *Lecture Notes in Computer Science*. Springer Berlin / Heidelberg, 2010, pp. 29–42.

[98] VRŠEK, J., AND LÁVIČKA, M. On convolutions of algebraic curves. *Journal of symbolic computation 45*, 6 (2010), 657–676.

[99] ŠÍR, Z., BASTL, B., AND LÁVIČKA, M. Hermite interpolation by hypocycloids and epicycloids with rational offsets. *Computer Aided Geometric Design 27* (2010), 405–417.

[100] ŠÍR, Z., AND JÜTTLER, B. Euclidean and Minkowski Pythagorean hodograph curves over planar cubics. *Comput. Aided Geom. Des. 22*, 8 (2005), 753–770.

[101] ŠÍR, Z., AND JÜTTLER, B. Spatial Pythagorean hodograph quintics and the approximation of pipe surfaces. In *The Mathematics of Surfaces XI* (2005), Springer, pp. 364–380.

[102] ŠÍR, Z., AND JÜTTLER, B. C^2 Hermite interpolation by Pythagorean hodograph space curves. *Mathematics of Computation 76* (2007), 1373–1391.

[103] WALTON, D., AND MEEK, D. Curve design with a pair of Pythagorean hodograph quintic spiral segments. *Computer Aided Geometric Design 24*, 5 (2007), 267–285.

[104] WALTON, D. J., AND MEEK, D. S. A pythagorean hodograph quintic spiral. *Computer-Aided Design 28*, 12 (1996), 943–950.

[105] WANG, G., AND FANG, L. On control polygons of quartic pythagorean-hodograph curves. *Computer Aided Geometric Design 26*, 9 (2009), 1006–1015.